Conference on Modelling Fluid Flow (CMFF'22)
The 18th International Conference on Fluid Flow Technologies
Budapest, Hungary, August 30-September 2, 2022

On the Effect of Mass Fraction of Frozen Mixture Flow on the Dynamic Performance of a Direct Spring Operated Safety Valve

Csaba Hős[1], G. Burhani[2]

[1] Corresponding Author. Department of Hydrodynamic Systems, Faculty of Mechanical Engineering, Budapest University of Technology and Economics. Bertalan Lajos u. 4 - 6, H-1111 Budapest, Hungary. Tel.: +36 1 463 2216, E-mail: hos.csaba@gpk.bme.hu
[2] Department of Fluid Hydrodynamic Systems, Faculty of Mechanical Engineering, Budapest University of Technology and Economics.
E-mail: gburhani@hds.bme.hu

ABSTRACT

We study the effect of frozen mixture (constant mass fraction) flow through a pressure relief valve with upstream piping. DIER's omega technique is employed to cope with the mixture parameters, notable sonic velocity and choked/non-choked flow via the nozzle. By means of one-dimensional simulation, we show that the change in sonic velocity play a fundamental role in both the valve opening time and the its stability. Due to the extremely low sonic velocities e.g. in the case of water-air mixture, such valves will have a poor response time (slow opening) and will also chatter even for short inlet pipings.

Keywords: safety vale, frozen mixture, sonic velocity, valve chatter, valve opening time

NOMENCLATURE

$\mathcal{G}$	$[-]$	dimensionless mass flux
A_s	$[m^2]$	seat area
C_d	$[-]$	discharge coefficient
f	$[Hz]$	frequency
k	$[Ns/m]$	viscous damping coefficient
m	$[kg]$	mass of the valve
p	$[Pa]$	pressure
R	$[J/(kgK)]$	specific gas constant
s	$[N/m]$	spring stiffness
T	$[K]$	temperature
V	$[m^3]$	volume
x	$[m]$	valve displacement
x_0	$[m]$	spring pre-compression
$\dot{m}$	$[kg/s]$	mass flow rate
c	$[m/s]$	speed of sound
p	$[Pa]$	pressure
x	$[-]$	mass fraction
α	$[-]$	volume fraction
ω	$[rad/s]$	eigenfrequency
ρ	$[kg/m^3]$	density

Subscripts and Superscripts

a	ambient
b	back (pressure)
ft	flow-through (area)
g	gas
l	liquid
m	mixture
r	reservoir
ref	reference
set	set (pressure)
u	upstream
v	valve

1. INTRODUCTION

Pressure relief valves (PRV) are devices that protect the pipeline system and reservoirs from excess pressure by venting the unnecessary amount of fluid if needed. As such, they are safety-critical devices; inadequate operation (such as insufficient venting capacity, vibration, the inability of opening due to stuck parts) leads to catastrophic consequences.

These valves are essentially 1 DoF oscillators coupled with the fluid dynamics inside the piping system, resulting in a surprisingly rich dynamical behaviour, see e.g. [1] for an overview. It is well-known that such valves are prone to self-excited oscillations ([2, 3, 4, 5, 6]) and a significant effort was devoted to predicting such oscillations in the phase of design (see [7, 8, 9, 10]). One of the cornerstones of such an analysis is the high-fidelity, yet relatively simple description of the flow force on the valve body and the mass flow rate through the PRV. Although there are standard approaches of describing these forces – e.g. the 'effective area' technique introduced in [11] or the use of the jet angle as in [7, 12] – mostly single-phase cases (either pure gas or liquid) are addressed. [13, 14, 15, 12, 16] report on the effect of the two-phase flow on the *static* characteristics (flow force and mass flux) of the valve, however, the authors are unaware of any study trying to capture the effect of multiphase flow on the *dynamic* behaviour of the PRV, notably opening and closing characteristics.

This paper addresses the problem of predicting the dynamic behaviour of a PRV in the presence of two-phase flow of constant mass fraction. As such, we do not consider phase change and the model will not be (directly) applicable for systems where interphase mass transfer is present (e.g. flashing flows). However, for multicomponent applications, in the absence of mass transfer between the components, our model will provide a possible description of the dynamics, for example in the case of bubbly flows [17, 18, 19], where, even though the void fraction changes if pressure changes, the mass fraction remains constant. Another example with constant mass fraction would be applications in which the humidity content of air is important, see e.g. [20] or [21], especially Figure 8 therein.

In what follows, we start by providing a brief literature overview in section 2, then present our model in section 3. Next, we present our simulation results on the estimation of valve opening time in section 4 and valve stability in section 5. Finally, in section 6 concludes the study.

2. LITERATURE OVERVIEW

Industrial pressure relief valves are sized and chosen based on their capacity, that is the vented mass flow rate at full opening and 110% of the set (opening) pressure. For simple cases such as ideal gas or incompressible liquid, it is straightforward to compute the mass flow rate if the valve lift (flow-through area) and the pressure difference (or, in the case of choked flow, the upstream pressure) are known, together with the discharge coefficient (provided by the manufacturer). However, in the case of wet steam, non-ideal gases or mixtures, or flashing (partial evaporation of saturated liquid due to pressure drop via the valve), predicting the mass flow rate is challenging. DIER's ω technique is one attempt to cope with this problem, that assumes both thermal and mechanical homogeneous case and also neglects the velocity difference between the phases (no slip). Due to its popularity, we will employ this model, even though there are other, more accurate (and complex) models, such as TPHEM, HNE, and HDI methods (see [22] for details).

In contrast to the single-phase flow, the two-phase case has one additional degree of freedom, that is the mass fraction of one of the phases; that is gas mass fraction $x_g = m_g/(m_g + m_l)$ and the liquid mass fraction $x_l = \dot{m}_l/(\dot{m}_g + \dot{m}_l)$.

Leung published a series of papers on the development and use of the ω technique. In [23] he presented the generalised correlation for one-component homogeneous equilibrium model (HEM) for flashing choked flow validated against measurement results for eleven fluids with different properties. The key idea was that the flashing two-phase mixture was considered as a single-phase compressible fluid, and then the use of the ω parameter already defined by Epstein at al. in [24] for all-liquid mixtures. In [25] the same author with Grolmes extended the previous correlation for the flashing choked flow of an initially sub-cooled liquid (for both high and low sub-cooling regions), neglecting the effects of non-equilibrium effects and obtained design charts that were useful for practical applications. Leung discussed similarities between flashing and non-flashing two-phase flow in [26] and showed that, by simply redefining the dimensionless ω parameter, a unified treatment could be obtained.

In another study ([27]), Leung and Nazario reviewed three methods; (a) DIERS' ω method, (b) a technique used by the American Petroleum Institute (API) and (c) an ASME method, to compare the two-phase flashing flow prediction tools, which are highly used in various engineering applications. Their comparison showed that the ASME and DIERS (homogeneous equilibrium) models are in close agreement (these approaches assume isentropic expansion in the nozzles). Moreover, the API method gives significantly higher theoretical mass flux values since it neglects momentum, heat and mass transfer during the flashing process.

Leung summarised his previous work in [28], covering the ω method for mass flux estimation both for ideal nozzle flow and pipe flow with different orientations (horizontal and inclined pipe flows), for flashing, non-flashing, inlet sub-cooled and non-condensible gas. Nine years later, in 2004, Leung applied the ω method for safety relief valves in [29]. It was also shown how the discharge coefficient varies depending on the flow regime, and it was revealed that for the non-flashing flow case, the discharge coefficient lies between the liquid coefficient and the gas coefficient. Moreover, he also observed a higher discharge coefficient value in the case of flashing flow, compared to the single-gas case. In [30], the same author proposed techniques for employing the ω model based on the stagnation conditions of fluid in the vessel and discussed four main cases; saturated liquid, two-phase (gas-liquid mixture), low sub-cooled liquid, and high sub-cooled liquid.

In [31], Lenzing et al. studied the effect of two-phase flow (flashing and non-flashing) on the capacity (i.e. at maximum lift) of safety relief valve experimentally. They compared the measured data against several theoretical predictions; namely the Isentropic Homogeneous Equilibrium Model, DIERS' ω technique, Nastoll's Homogeneous Frozen Flow model and the Goßlau-Weyl model. One of the outcomes of this work is that for non-flashing two-component air/water flow Leung's, extended by the weighted discharge coefficient, can be used (see Figure 1. in [31] and the corresponding text).

Another experimental validation of the technique was reported by Gino Boccardi *et al.* in [32]. The authors compared the test data for steam-water flow in a safety relief valve against three prediction techniques, namely HEM (homogeneous equilibrium model), HNE (thermodynamic non-equilibrium) and

HNE-DS (proposed by the ISO working group), to predict the theoretical mass flux. The results revealed that, even though the HNE-DS method provided the best results, it was not conservative in the sense that in some cases, it predicted higher flow rates compared to the measurements. In contrast, the HEM technique gave poor accuracy, but it was conservative. The same author in a later work [13] discussed another set of experimental data on (steam/water) flashing system through a PRV with a wide range of the operating parameters (such as vapour quality, inlet pressure, mass flow rate, and backpressure). These measurements were also tested against the predictions of the HEM ω method, and the results showed that the mass flow rates provided by the theoretical model and the actual (measured) flow rates correlated reasonably.

Based on the theoretical and experimental work published in the above reports, Leung's ω technique provides a reasonable compromise between modelling complexity and prediction accuracy and we will employ this approach in this paper.

3. MODELLING

3.1. Frozen mixture model

Consider the frozen mixture of an ideal gas and a liquid, that is the gas *mass* fraction $x_g = \frac{m_g}{m_m} = \frac{\dot{m}_g}{\dot{m}_m}$ is constant, where $\dot{m}_m = \dot{m}_g + \dot{m}_l$ and, clearly, $x_l = 1 - x_g$.

We assume that the gas obeys the ideal gas law, that is $p/\rho_g = RT$. For an isentropic change of state, the sonic velocity for *pure gas* ($x_g = 1$) is $c_g = \sqrt{\kappa RT}$. The equation of state of the liquid phase is

$$\rho_l = \rho_{ref} + \frac{1}{c_l^2}\left(p - p_{ref}\right), \tag{1}$$

where the reference values are $p_{ref} = 1\text{bar}$ and $\rho_{ref} = 1000\,kg/m^3$ and c_l is the sonic velocity measured in pure liquid.

The α volume fraction is

$$\alpha_g = \frac{V_g}{V_g + V_m} = \frac{m_g}{m_g + m_l\frac{\rho_g}{\rho_l}} = \frac{x_g}{x_g + (1 - x_g)\frac{\rho_g}{\rho_l}}, \tag{2}$$

with which the mixture density $\rho_m(p, T, x_g)$ becomes

$$\begin{aligned}\rho_m &= \frac{m_m}{V_m} = \frac{\rho_g V_g + \rho_l V_l}{V_g + V_l} = \alpha\rho_g + (1 - \alpha)\rho_l \\ &= \frac{p\left(p - p_{ref} + c_l^2\rho_{ref}\right)}{(p_{ref} - p)RTx_g + c_l^2\left(p(x_g - 1) - RTx_g\rho_{ref}\right)}\end{aligned} \tag{3}$$

It is easy to check that $\rho_m(x_g = 0) = \frac{p}{RT}$ and setting $x_g = 1$ recovers (1). We will also need the pressure as a function of temperature, (mixture) density and gas mass fraction $p(\rho_m, T, x_g)$, which is

$$\begin{aligned}p &= \frac{1}{4}\left(-b + \sqrt{b^2 - 4c}\right), \quad \text{width} \\ b &= -\left(p_{ref} + RTx_g\rho_m + c_l^2\left(\rho_m(1 - x_g) - \rho_{ref}\right)\right) \quad \text{and} \\ c &= RTx_g\rho_m\left(p_{ref} - c_l^2\rho_{ref}\right).\end{aligned} \tag{4}$$

Now we are in the position of computing the mixture sonic velocity, that will play a central role in our later analyses. First, we eliminate the temperature dependence from (3) by assuming isentropic change of state for the gas, and then compute

$$\begin{aligned}c_m^2 &= \left(\frac{\mathrm{d}\rho_m(p, x_g)}{\mathrm{d}p}\right)^{-1}\Bigg|_{isentropic} \\ &= \frac{\kappa\,(a_0 + a_1)^2}{b_0 + b_1 + b_2 + b_3} \quad \text{where} \\ p &= p_{ref,g}\left(\frac{T}{T_{ref,g}}\right)^{\frac{\kappa}{\kappa-1}} \\ a_0 &= (p - p_{ref})RTx_g \\ a_1 &= c_l^2\left(p(1 - x_g) + RTx_g\rho_{ref}\right) \\ b_0 &= -p^2RTx_g \\ b_1 &= c_l^2p^2(x_g - 1) \\ b_2 &= 2pRTx_g\left(p_{ref} - c_l^2\rho_{ref}\right) \\ b_3 &= -RTx_g\left(p_{ref} - c_l^2\rho_{ref}\right)^2\end{aligned} \tag{5}$$

It straightforward again to check that $c_s^2(x_g = 0) = c_l^2$ and $c_s^2(x_g = 1) = \kappa RT$. Figure 1 depicts the change of sonic velocity (solid line) and gas void fraction α_g (dashed line) as a function of gas mass fraction. These results are in good agreement with the literature data, see [33] for example. The sonic velocity will a play a central role in our further analysis, hence we highlight two well-known facts, namely that (a) it can be as low as 20-50 m/s and (b) a relatively small amount of air (say, $x_g = 10^{-6}$, $\alpha_g = 8.3 \times 10^{-4}$) changes the sonic velocity drastically.

3.2. Pipe flow modelling

The governing equations for the 1D, unsteady flow of an arbitrary fluid in a tube of constant cross section (that is, a pipe) can be written as

$$\frac{\partial\mathcal{U}}{\partial t} + \frac{\partial\mathcal{F}}{\partial x} = \mathcal{S}, \tag{6}$$

with

$$\mathcal{U} = \begin{pmatrix}\rho_m \\ \rho_m v \\ \rho_m v e_{tot}\end{pmatrix}, \quad \mathcal{F} = \begin{pmatrix}\rho_m v \\ \rho_m v^2 + p \\ \rho_m v e_{tot} + pv\end{pmatrix}, \quad \text{and} \tag{7}$$

$$\mathcal{S} = \begin{pmatrix}0 \\ -\frac{\lambda}{2d}v|v| \\ 0\end{pmatrix}. \tag{8}$$

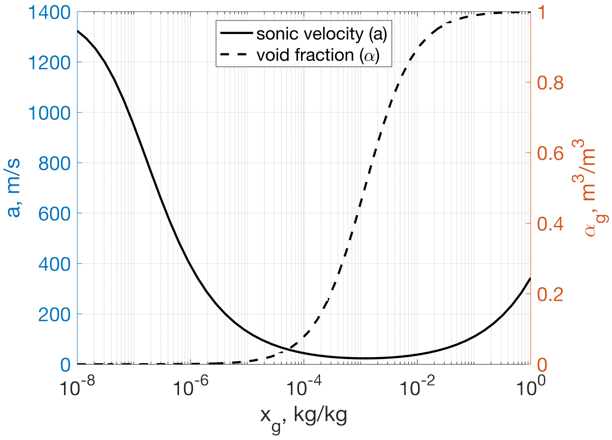

Figure 1. Sonic velocity (left axis) and gas void fraction (right axis) as a function of gas mass fraction.

where $e_{tot} = e + \frac{v^2}{2}$ and the mixture internal energy is $e_m = e_g + e_l = c_{V,g}Tx_g + c_lT(1-x_g) = c_{V,m}T$, where the mixture specific heat capacity at constant volume is $c_{V,m} = x_g c_{V,g} + c_l(1-x_g)$.

3.3. Valve model

The valve is modelled by a simple 1 DoF oscillatory system, whose governing equation is given by

$$m_v\ddot{x} + k\dot{x} + s(x + x_0) = \tilde{A}_{eff}(x)A_s(p_u - p_b). \quad (9)$$

$\tilde{A}_{eff}$ is the dimensionless *effective area* curve, which models the force component due to the momentum of the fluid (see [34, 35] for more details). The pressure difference $p_u - p_b$ contains the upstream pressure and the backpressure, which does not necessarily equal the ambient pressure p_a. By adjusting the x_0 spring pre-compression, one can change the opening or *set pressure* p_{set}, which, by definition, is a gauge pressure: $p_{set} = \frac{sx_0}{A_s} - p_a$. Pressure relief valves in oil and gas industry typically contain no artificial damping mechanism but only natural damping, hence we will set $k = 0.01k_{crit} = 0.01 \times 2\sqrt{sm}$.

The mass flow rate through the valve is $\dot{m} = C_dA_{ft}(x)\sqrt{p_u\rho_u}\mathcal{G}(\eta)$. The *dimensionless* mass flux $\mathcal{G}$ is ($\eta = p_d/p_u$)

for an incompressible fluid:

$$\sqrt{2(1-\eta)} \quad (10)$$

for an un-chooked, single-phase ideal gas:

$$\sqrt{2\frac{\kappa}{\kappa-1}\left(\eta^{2/\kappa} - \eta^{(\kappa+1)/\kappa}\right)} \quad (11)$$

for a choked, single-phase ideal gas:

$$\sqrt{\kappa\left(\frac{2}{\kappa+1}\right)^{\frac{\kappa+1}{\kappa-1}}} \quad (12)$$

for an un-choked frozen mixture fluid:

$$\frac{(-2(\omega\ln\eta + (\omega-1)(1-\eta))^{1/2}}{\omega(\frac{1}{\eta}-1)+1} \quad (13)$$

for a choked frozen mixture fluid:

$$\frac{\eta_c}{\sqrt{\omega}}, \quad (14)$$

where the critical pressure ratio $\eta_c = \frac{p_c}{p_0}$ can be calculated by solving the following implicit equation:

$$\eta_c^2 + (\omega^2 - 2\omega)(1-\eta_c)^2 + 2\omega^2\ln\eta_c + 2\omega^2(1-\eta_c) = 0. \quad (15)$$

and $\omega = \alpha_g/\kappa$, see [28].

3.4. Reservoir model

The rate of change of pressure inside a reservoir is

$$\dot{p}_t = \frac{a_r^2}{V}(\dot{m}_{in} - \dot{m}_{out}). \quad (16)$$

We shall assume constant inlet flow rate $\dot{m}_{in}$ and variable outlet flow rate, typically, through a pipeline. The reservoir sonic velocity a_r depends on the reservoir temperature, which is connected to the reservoir pressure p_r by an arbitrary, user-defined change of state (e.g. isentropic, isotherm, etc).

3.5. Numerical solution procedure

We use a standard Lax-Wendroff scheme for updating the pipe. The boundary conditions are implemented with the help of Method of Characteristics (MoC, see [36]), the details can be found in [37]. The valve and reservoir model are integrated by a standard 5th-order adaptive Runge-Kutta solver. Special care is devoted to the proper handling of the valve impingement on the seat or upper stopper. The time step is chosen by the CFL criteria, with a CFL number of 0.7-0.9. The whole framework is implemented in Matlab 2021b.

4. VALVE OPENING TIME

In [34], an approximate formula was derived for 'fast' valves. Let the timescale of the valve be $t_{valve} = 2\pi/\omega_v = 2\pi\sqrt{m/s}$. We define the opening time t_{op} as the time needed for a *closed* valve to reach the 95% of the equilibrium lift x_e for a prescribed mass flow rate $\dot{m}_{in}$. If $t_{op} \ll t_{valve}$, we have

$$t_{op} \approx 2 \times 0.95 x_e \omega_v^2 \frac{m\sum V}{A_s a^2 \dot{m}_{in}}. \quad (17)$$

(The condition $t_{op} \ll t_{valve}$ or, equivalently, $\omega_v t_{op} \ll 2\pi$ must be checked a posteriori.) The above equation was derived by assuming a valve mounted directly to the reservoir. Intuitively, a pipe between the valve and reservoir would add addition volume and, if long enough, it will give rise to wave phenomena that also increases the valve opening time, hence we have $\sum V = V_r + A_pL_p$.

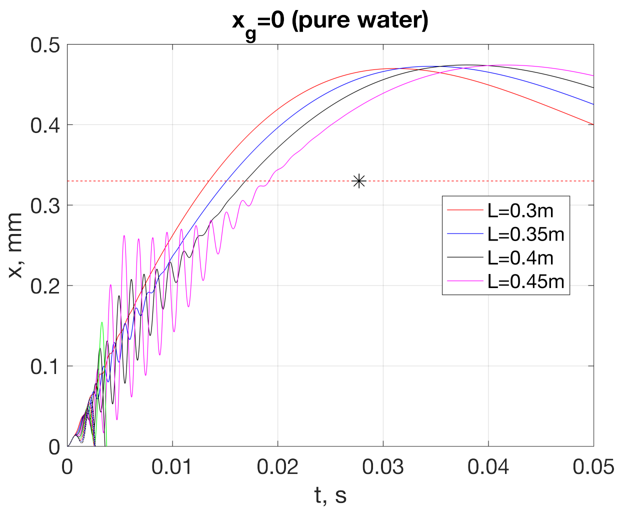

Figure 2. Valve openings with different pipe lengths, for pure water. The dashed line represents the equilibrium lift, the asterisk depict the opening time estimates by (17)**.**

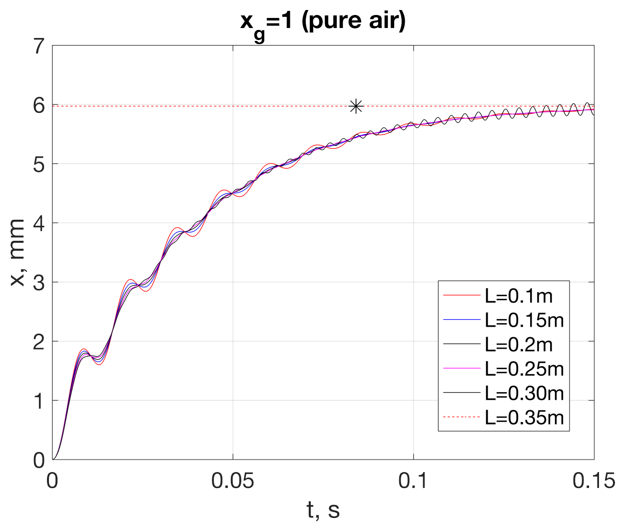

Figure 3. Valve openings with different pipe lengths, for pure air. The dashed line represents the equilibrium lift, the asteriks depict the opening time estimates by (17)**.**

We have run several computations to analyse the effect of mass fraction on the valve opening time with the parameter values provided in Table 1. For the water case, we have set $V = 2\text{m}^3$ and the equilibrium position was $x_e = 0.33$mm and $p_e = 4.11$ bara. This gives (by virtue of (17)) $t_{op} = 0.0278$ s for opening time. Figure 2 depicts the first 0.05 s of the opening process with three different pipe lengths. The dashed horizontal line represents the equilibrium valve lift and the asterisk is the estimates opening time. We observe a slightly increasing opening time due to the increasing pipe length, which changes the overall volume (capacity) in the system. The change in the opening time ((17)) due to the increasing pipe length is less than 1%. We also experienced "opening instability" (see [11] for details). From the mechanical point of view, this case is underdamped as the maximum of the valve lift is 50% higher than the equilibrium position.

Table 1. Parameters

valve mass	m	0.2 kg
spring stiffness	s	47.3 kN/m
valve eigenfreq.	f_v	77 Hz
valve timescale	t_v	0.013 s
set pressure	p_{set}	3 barg
pipe diameter	D_p	45.5 mm
pipe friction coeff.	λ	0.02
inlet mass flow rate	$\dot{m}_{in}$	0.77 kg/s

In the case of pure air, we have $V = 0.02\text{m}^3$, $x_e = 5.97$mm and $p_e = 5.9$bara. This case is overdamped, even though the viscous damping parameter was unchanged and the reservoir volume is smaller. Again, the dashed line represents the equilibrium lift, the asterisk depict the opening time estimates by (17). In this case, we do not experience opening instability.

In both cases, the simulations with longer pipe lengths resulted in unstable valve motion, leads us to our next section.

5. STABILITY AND VALVE CHATTER

In [38], the authors derived an analytical criteria for computing the critical inlet pipe length, that is

$$L_{crit} = \frac{\pi a}{2\omega_v} \frac{1}{\sqrt{2\frac{A_v p_e}{x_e s} + 1}}, \tag{18}$$

where x_e and p_e are the equilibrium valve lift and (absolute) pressure at the valve inlet. Beyond the critical pipelength defined by the above equation, self-excited oscillations will be born, whose dominant frequency will coincide with the pipe's first natural 'organ-mode' eigenfrequency, $f_p = a/(4L)$.

Izuchi in [9] provided a similar equation, that is

$$L^*_{crit} = \frac{\pi a}{2\omega_v} \frac{1}{\sqrt{\frac{x_e + x_0}{x_e}}}. \tag{19}$$

We notice that due to the force equilibrium of the valve, we have $s\,(x_e + x_0) = A_v\,(p_u - p_b)$, hence, if p_u is measured as a *relative* (gauge) pressure above p_b (which is often the ambient pressure), and the momentum forces can be neglected ($A_{eff} = 1$ in (9)), we have $\frac{A_v p_e}{x_e s} = \frac{x_e + x_0}{x_e}$, which is similar to Izuchi's equation, but still, the factor of 2 and the +1 terms are missing.

We have run simulations with two set pressure, that is $p_{set} = 3$ barg and 10 barg. Figures 4 and 5 depict the result. As it can be seen by virtue of (18), the critical pipe length depends on the equilibrium lift and pressure (x_e and p_e) and the sonic velocity. The uppermost panels show the equilibrium lift: it remains constant up to $x_g \approx 0.01$, beyond which it

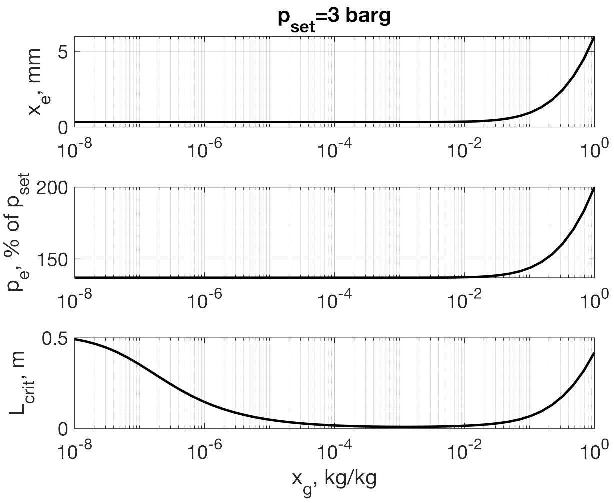

Figure 4. Equilibrium lift, pressure and critical pipe length for $p_{set} = 3$ barg and $\dot{m}_{in} = 0.77$ kg/s.

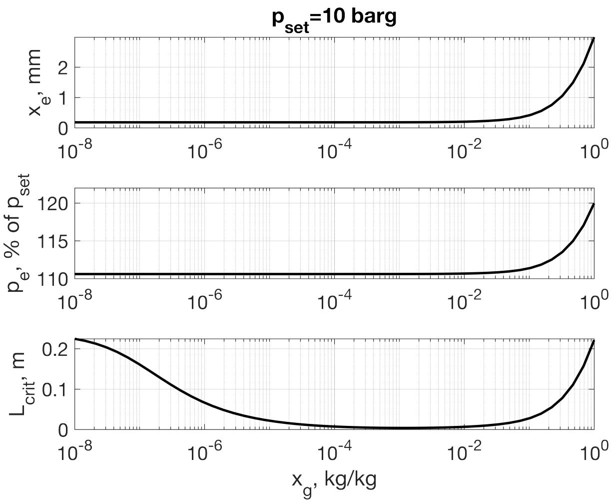

Figure 5. Equilibrium lift, pressure and critical pipe length for $p_{set} = 10$ barg and $\dot{m}_{in} = 0.77$ kg/s.

increases due to the fact that the density of the mixture decreases but the overall vented mass flow rate is kept constant. We observe a similar trend in the case of the equilibrium pressure.

However, the shape of the critical pipe length (bottom panels) resembles on the shape of the sonic velocity, see Figure 1. More importantly, in the range of $x_g < 10^{-2}$, the equilibrium lift and pressure are constant yet the critical pipe length changes. This is another observation supporting the importance of the sonic velocity. Again, in the range of the low sonic velocity, the valve will be unstable basically for any (small) pipe length.

6. SUMMARY AND CONCLUSION

We have shown the importance of sonic velocity on valve stability and opening time. Lower sonic velocities will result in slow valve motions and highly unstable valve operation. Our numerical tests has shown that both formulae (opening time (17) and critical pipe length (18)) provide simple means for an order-of-magnitude estimation even in the case of mixture flow. This study was the precursor of further investigation towards exploring the possibility of predicting valve dynamics and stability in the case of non-ideal and/or flashing fluids.

REFERENCES

[1] Hős, C. J., Champneys, A. R., Paul, K., and McNeely, M., 2017, "Dynamic behaviour of direct spring loaded pressure relief valves connected to inlet piping: IV review and recommendations", *Journal of Loss Prevention in the Process Industries*, Vol. 48, pp. 270–288.

[2] Kasai, K., 1968, "On the Stability of a Poppet Valve with an Elastic Support", *Bulletin of JSME*, Vol. 11 (48).

[3] Bazsó, C., and Hős, C., 2013, "An experimental study on the stability of a direct spring loaded poppet relief valve", *Journal of Fluids and Structures*, Vol. 42, pp. 456–465.

[4] Moussou, P., Gibert, R. J., Brasseur, G., Teygeman, C., Ferrari, J., and Rit, J. F., 2010, "Instability of Pressure Relief Valves in Water Pipes", *Journal of Pressure Vessel Technology*, Vol. 132 (4), p. 041308.

[5] Singh, A., 1983, "On the stability of a coupled safety valve-piping system.", *IN: Thermal-hydraulics of nuclear reactors, paper presented at the second int topical meeting on nuclear reactor thermal-hydraulics*.

[6] Singh, A., 1982, "An analytical study of the dynamics and stability of a spring loaded safety valve", *Nuclear Engineering and Design*, Vol. 72 (2), pp. 197–204.

[7] Darby, R., 2012, "The dynamic response of pressure relief valves in vapour or gas service. Part 1: mathematical model", Proprietrary report for PERF 99-05.

[8] Hős, C., Champneys, A., Paul, K., and McNeely, M., 2014, "Dynamic behavior of direct spring loaded pressure relief valves in gas service: Model development, measurements and instability mechanisms", *Journal of Loss Prevention in the Process Industries*, Vol. 31, pp. 70–81.

[9] Izuchi, H., 2010, "Stability Analysis of Safety Valve", American Institute of Chemical Engineers, *10th Topical Conference on Natural Gas Uitilization ISBN: 9781617384417*.

[10] Melham, G., 2014, "Analysis of PRV Stability in Relief Systems, Part I. Detailed Dynamics", An ioMosaic Corporation White Paper.

[11] Hős, C. J., Champneys, A. R., Paul, K., and McNeely, M., 2014, "Dynamic behavior of direct spring loaded pressure relief valves in gas service: Model development, measurements and instability mechanisms", *Journal of Loss Prevention in the Process Industries*, Vol. 31 (1), pp. 70–81.

[12] Narabayashi, T., Nagasaka, H., Niwano, M., and Ohtsuki, Y., 1986, "Safety relief valve performance for two-phase flow", *Journal of Nuclear Science and Technology*.

[13] Boccardi, G., Bubbico, R., Celata, G., and Mazzarotta, B., "Two-phase flow through pressure safety valves. Experimental investigation and model prediction", *Chemical Engineering Science*, (19), pp. 5284–5293.

[14] Dempster, W., and Alshaikh, M., 2015, "An Investigation of the Two Phase Flow and Force Characteristics of a Safety Valve", Tu, ST and Chen, X (ed.), *Pressure Vessel Technology: Preparing For the Future*, Vol. 130 of *Procedia Engineering*, pp. 77–86.

[15] Kourakos, V., Rambaud, P., Buchlin, J. M., and Chabane, S., 2013, "Flowforce in a safety relief valve under incompressible, compressible, and two-phase flow conditions (PVP-2011-57896)", *Journal of Pressure Vessel Technology, Transactions of the ASME*.

[16] Dempster, W., and Alshaikh, M., 2015, "An Investigation of the Two Phase Flow and Force Characteristics of a Safety Valve", *Procedia Engineering*, Vol. 130, pp. 77 – 86.

[17] van Lookeren Campagne, C., Nicodemus, R., de Bruin, G. J., and Lohse, D., 2002, "A Method for Pressure Calculation in Ball Valves Containing Bubbles ", *Journal of Fluids Engineering*, Vol. 124 (3), pp. 765–771.

[18] Ng, K., and Yap, C., 1989, "An investigation of pressure transients in pipelines with two-phase bubbly flow", *International journal for numerical methods in fluids*, Vol. 9 (10), pp. 1207–1219.

[19] Alimonti, C., Falcone, G., and Bello, O., 2010, "Two-phase flow characteristics in multiple orifice valves", *Experimental thermal and fluid science*, Vol. 34 (8), pp. 1324–1333.

[20] Meena, P., Rittidech, S., and Poomsa-ad, N., 2007, "Application of closed-loop oscillating heat-pipe with check valves (CLOHP/CV) air-preheater for reduced relative-humidity in drying systems", *Applied Energy*, Vol. 84 (5), pp. 553 – 564.

[21] Kim, D. K., Min, H. E., Kong, I. M., Lee, M. K., Lee, C. H., Kim, M. S., and Song, H. H., 2016, "Parametric study on interaction of blower and back pressure control valve for a 80-kW class PEM fuel cell vehicle", *International Journal of Hydrogen Energy*, Vol. 41 (39), pp. 17595 – 17615.

[22] Darby, R., 2005, "Size safety-relief valves for any conditions", *Chemical Engineering*, Vol. 112 (9), pp. 42–50.

[23] Leung, J., 1986, "A generalized correlation for one-component homogeneous equilibrium flashing choked flow", *AIChE Journal*, Vol. 32 (10), pp. 1743–1746.

[24] Epstein, M., Henry, R., Midwidy, W., and Pauls, R., 1983, "One-Dimensional Modeling of Two-Phase Jet Expansion and Impingement", *Proc. of the 2nd Int. Topical Meet. Nuclear Reactor Thermal-Hydraulics*.

[25] Leung, J. C., and Grolmes, M. A., 1988, "A generalized correlation for flashing choked flow of initially subcooled liquid", *AIChE Journal*, Vol. 34 (4), pp. 688–691.

[26] Leung, J. C., 1990, "Similarity between flashing and nonflashing two-phase flows", *AI Ch E Journal (American Institute of Chemical Engineers);(USA)*, Vol. 36 (5).

[27] Leung, J., and Nazario, F., 1990, "Two-phase flashing flow methods and comparisons", *Journal of Loss Prevention in the Process Industries*, Vol. 3 (2), pp. 253–260.

[28] Leung, J., 1995, "The Omega Method for Discharge Rate Evaluation", *International symposium, Runaway reactions and pressure relief design*, DIERS, AICHE, The address of the publisher, pp. 367–393, iSBN: 0816906769.

[29] Leung, J., "A theory on the discharge coefficient for safety relief valve", *Journal of Loss Prevention in the Process Industries*, (4), pp. 301–313.

[30] Lees, F., 2012, *Lees' Loss prevention in the process industries: Hazard identification, assessment and control*, Butterworth-Heinemann.

[31] Lenzing, T., Friedel, L., Cremers, J., and Alhusein, M., 1998, "Prediction of the maximum full lift safety valve two-phase flow capacity", *Journal of Loss Prevention in the Process Industries*, Vol. 11 (5), pp. 307–321.

[32] Boccardi, G., Bubbico, R., Celata, G. P., Di Tosto, F., and Trinchieri, R., 2010, "Comparison among three prediction methods for safety valves design in two-phase flow in the case of a small valve", *Chemical Engineering Transactions*, Vol. 19, pp. 175–181.

[33] Nguyen, D., Winter, E., and Greiner, M., 1981, "Sonic velocity in two-phase systems", *International Journal of Multiphase Flow*, Vol. 7 (3), pp. 311–320, URL https://www.sciencedirect.com/science/article/pii/0301932281900240.

[34] Burhani, M. G., and Hős, C., 2020, "Estimating the opening time of a direct spring operated pressure relief valve in the case of multiphase flow of fixed mass fraction in the absence of piping", *Journal of Loss Prevention in the Process Industries*, Vol. 66, pp. 104–169, URL https://www.sciencedirect.com/science/article/pii/S095042302030022X.

[35] 2021, "An Experimental Study on the Force Coefficient and the Discharge Coefficient of a Safety Valve in Air-water Mixture Flow", *PERIODICA POLYTECHNICA-MECHANICAL ENGINEERING*, Vol. 65, pp. 326–336.

[36] Anderson, J., 1995, *Computational Fluid Dynamics*, Computational Fluid Dynamics: The Basics with Applications, McGraw-Hill Education, ISBN 9780070016859, URL https://books.google.hu/books?id=dJceAQAAIAAJ.

[37] Erdődi, I., and Hős, C., 2017, "Prediction of quarter-wave instability in direct spring operated pressure relief valves with upstream piping by means of CFD and reduced order modelling", *Journal of Fluids and Structures*, Vol. 73, pp. 37–52, URL https://www.sciencedirect.com/science/article/pii/S0889974616303784.

[38] Hős, C., Champneys, A., Paul, K., and McNeely, M., 2016, "Dynamic behaviour of direct spring loaded pressure relief valves: III valves in liquid service", To appear in *Journal of Loss Prevention in the Process Industries*.